http://dx.doi.org/10.18462/iir.nh3-co2.2017.0039

PAPER ID XXXXX

PHASE CHANGE MATERIAL THERMAL ENERGY STORAGE FOR A LARGE AMMONIA CHILLER/HEAT PUMP SYSTEM

M. JOKIEL[(a)], H. KAUKO[(b),*], C. SCHLEMMINGER[(c)], A. HAFNER[(d)], I. C. CLAUSSEN[(b)]

[(a)]Technische Universität (TU) Braunschweig, Faculty of Mechanical Engineering, Schleinitzstraße 20, 38106 Braunschweig, Germany

[(b)]SINTEF Energy Research, Kolbjørn Hejes vei 1 B, 7491 Trondheim, Norway

[(c)]SINTEF Byggforsk, Høgskoleringen 7 B, 7491 Trondheim, Norway

[(d)]Norwegian University of Science and Technology (NTNU), Department of Energy and Process Engineering, Kolbjørn Hejes vei 1 D, 7491 Trondheim, Norway

*hanne.kauko@sintef.no, tel. +47 968 766 51

ABSTRACT

Thermal energy storage (TES) can be applied to reduce peak heating and cooling loads in buildings and to improve the performance and reliability of the heat supply system. For short-term TES, phase change materials (PCM) are a compact and efficient alternative. At the Bergen University College in Norway, three ammonia chillers/heat pumps cover the base load for heating and cooling. To reduce the required chiller capacity, PCM cold storage tanks have been installed. The present study evaluates the PCM-TES system in detail through modelling and analysis of measurement data. To gain more understanding of the freezing and melting processes, a dynamic model for the PCM-TES was developed in Dymola. The simulation results were validated towards measurement data. The model allows better understanding of the heat transfer characteristics of the PCM-TES, and enables more sophisticated dimensioning and design of future PCM-TES systems.

Keywords: Building heating and cooling systems; ammonia heat pumps; thermal energy storage; phase change material

1. INTRODUCTION

Buildings account for approximately 40 % of the energy consumption in the EU, and the demand is expected to increase with the growth in population and increasing requirements for building services and comfort (Pérez-Lombard, Ortiz et al. 2008). Significant energy efficiency improvements are required to reduce the energy demand of buildings, and, hence, the climate gas emissions. Thermal energy storage (TES) has been recognized as one of the most efficient ways to enhance the energy efficiency and sustainability of heating and cooling systems (Liu, Su et al. 2016). Energy storage is essential whenever there is a mismatch between the supply and consumption of energy. In many commercial buildings in particular, such as offices and educational buildings, substantial amounts of surplus heat is available due to the high cooling load created by solar radiation, computer facilities and people. In order to utilize the surplus heat upon demand, available surplus heat is stored using TES, which is crucial in reducing peak heating and cooling demands, and hence, the installation costs.

Phase change materials (PCM) are an appropriate form of TES for improving buildings energy efficiency (Regin, Solanki et al. 2008). Due to the high amount of latent heat released during phase change processes, large amounts of energy can be stored in relatively small volumes. Furthermore, the heat absorption and release take place at a constant temperature. The present study presents the modelling and analysis of a PCM-TES system installed at the Bergen University College (Norway).

Proper designing of the TES systems using PCM is challenging, and requires quantitative information about the heat transfer and phase change processes in PCM (Regin, Solanki et al. 2008). For this purpose, models of the storage systems and simulations of their performance are required to be able to make assumptions and predictions on the design, dimensioning and layout of storage units. With the help of an appropriate model, the

http://dx.doi.org/10.18462/iir.nh3-co2.2017.0039

dynamic behaviour of the system can be examined for several boundary conditions, and for different sets of system parameters (Hed and Bellander 2006). This addresses challenges related to real world test rigs, which are cost intensive and require lots of space, and are locked to certain system specifications.

2. PCM STORAGE SYSTEM AT BERGEN UNIVERSITY COLLEGE

Three high-efficient ammonia chillers/heat pumps cover the base load for heating and cooling at the Bergen University College. The total installed cooling capacity is 1400 kW. The heat pump units are equipped with variable speed piston compressors and plate-and-shell heat exchangers. To reduce the required chiller capacity, a PCM cold storage system with a total cooling capacity of 1600 kW (11 200 kWh) at 10 °C has been installed. In addition, a borehole park consisting of 81 boreholes, each 220 m deep, is applied for seasonal TES.

The PCM-TES system consists of four PCM cold storage tanks (Figure 1 (a)), of about 60 m^3 each. The tanks are filled with PCM containers that contain salt hydrate (Figure 1 (b)), with a phase change temperature of 10 °C (PCM Products Ltd. 2011). The peak cooling demand of the university college is estimated to 3000 kW, and with the installation of the PCM cold storage and evaporative cooling, the installed chiller capacity could be drastically reduced (Dar 2014).

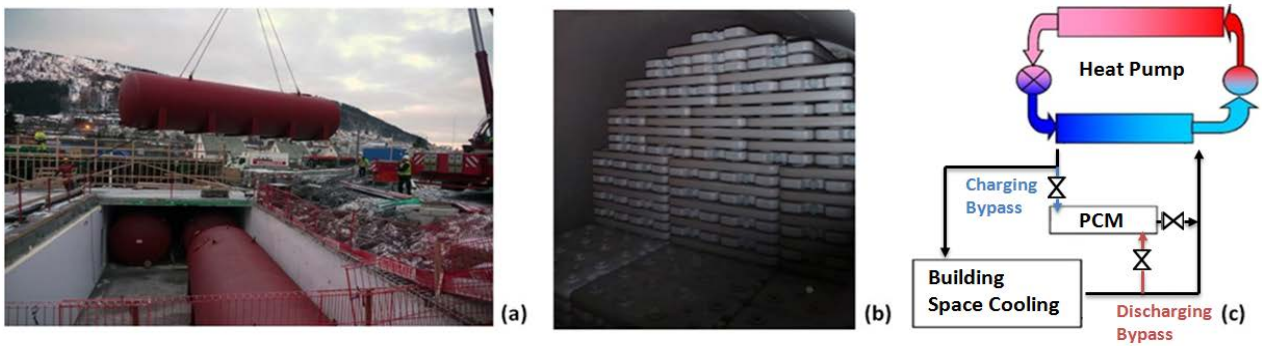

Figure 1 – (a) PCM cold storage tank installation at Bergen University College, (b) PCM containers within the tank and (c) a simplified system diagram of the chilled water distribution loop (Dar 2014)

The tanks are connected to the chilled water distribution loop (Figure 1 (c)) and act as a peak cooling device. During operation, water flows through the tanks and through the small flow passages between the stacked PCM containers. Two different operation modes can be distinguished: (1) During charging (freezing of the PCM), chilled water supplied by the heat pump/chiller unit flows into the PCM tanks. The charging mode is initiated if the inlet supply water temperature reaches a low level or if the cooling demand of the building is reduced, for example during night time. (2) During discharging (melting of the PCM), the PCM tanks are fed by warm return water from the space cooling loop. Without the PCM storage, cooling of the warm return water would result in an increased power demand in the heat pump/chiller unit.

3. MODELING THE PHASE CHANGE MATERIAL STORAGE

3.1 Derivation of the model

The PCM storage model has been implemented in Dymola using already existing Modelica libraries, TIL and TIL Media. TIL is a model library for thermal components and systems, while TIL Media contains a model library including thermophysical properties for the utilized fluids (TLK-Thermo GmbH 2016). The derived model consists simply of the PCM tank and inlet and outlet boundaries for the water. Since the PCM storage is essentially just exchanging heat with water flowing through it, the starting point was a simple fin and tube heat exchanger (HX) model modified and extended to represent a PCM cold storage.

The actual PCM storage is cylindrical. Figure 2 illustrates the steps of transforming the actual setup of stacked PCM containers in a cylindrical tank to a setup that resembles an ordinary rectangular HX structure. A square

http://dx.doi.org/10.18462/iir.nh3-co2.2017.0039

cross-sectional area allows a simpler calculation of mass flow and heat transfer rates in the model. After the PCM containers have been stacked in a compact way inside the tank, a cross-sectional area as shown in Figure 2 (b) is formed. Figure 2 (c) assumes that the walls between individual containers arranged side by side can be neglected, resulting in wide, flat and narrow water flow channels. The final form shown in Figure 2 (d) is derived by transforming the formerly round cross-section of the tank into a square one while the cross-sectional area is kept constant.

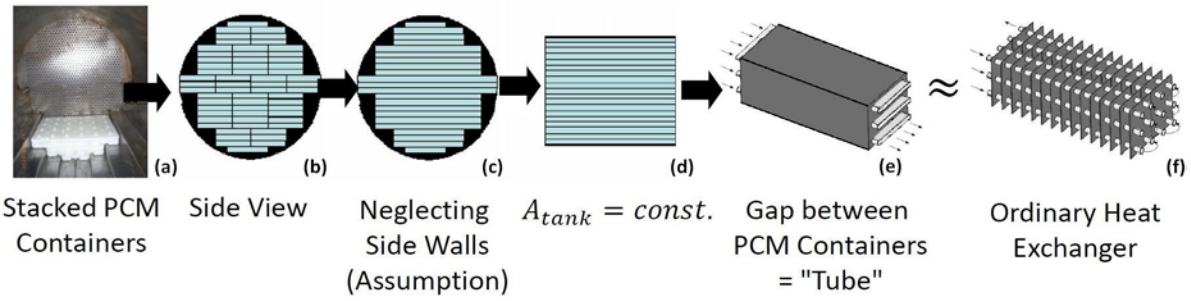

Figure 2 – Derivation of the model: Transforming stacked PCM containers to a rectangular flow channel structure that resembles ordinary heat exchangers (PCM Products Ltd. 2011, modified)

To be able to apply an existing HX model for the modified, rectangular PCM tank model, the following assumptions were made: (i) Flat rectangular flow ducts are used within the HX instead of ordinary round pipes (Figure 2 (e)). (ii) The walls of the flow channels are the walls of the PCM containers. (iii) A mass flow is only existent on the water side. (iv) The PCM side of the HX is a closed system with a constant mass. (v) No additional geometries such as fins are applied in the PCM HX; the heat transfer occurs only between the boundaries of "water to container wall" and "container wall to PCM". (vi) Heat transfer to the surroundings is neglected.

3.2 Model Structure

The PCM HX model estimates the heat transfer rate between a layer of PCM containers and the half of its surrounding flow channel on each container side. Figure 3 shows a system diagram with the boundaries for the model. It is assumed that water is equally distributed over the cross-sectional area, and the heat transfer rate will thus be the same for each container layer. The heat transfer rate is hence calculated for one layer only, and thereafter multiplied with the total number of flow channels to get the total heat transfer rate for the tank.

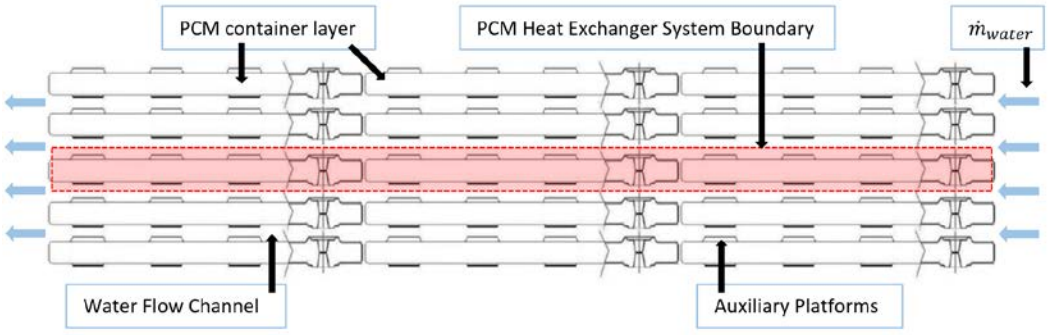

Figure 3 – Side view of the tank's internal scheme, showing water flow channels and the boundaries for a PCM HX model

The input parameters for the PCM storage model are given in Table 1. The values for the parameters were obtained from the product sheets for the PCM tank and the PCM containers (PCM Products Ltd. 2011). In addition to the parameters presented in Table 1, the measured outlet water temperature $T_{water,out}$ and the measured cooling capacity $\dot{Q}_{PCM}$ were utilized for validation (see section 4).

http://dx.doi.org/10.18462/iir.nh3-co2.2017.0039

Table 1 – Input parameter list for the PCM heat exchanger model

Discretization along the flow channel $n_{cells,flow\ channel}$	Discretization in direction of the PCM $n_{cells,PCM}$
Tank height h_{tank} [m]	Tank width b_{tank} [m]
Tank length l_{tank} [m]	Number of flow channels $n_{flow\ channels}$
Container wall thickness d_{wall} [m]	Flow channel height $h_{flow\ channels}$ [m]
Measured inlet water temp. $T_{water,in}$ [°C]	Measured mass flow rate $\dot{m}_{water}$ $[\frac{kg}{s}]$
Material properties of the PCM	Material properties of the wall (HDPE)

The PCM heat exchanger model consists of three different types of cells, shown in Figure 4 (a): PCM, liquid and wall cells. Liquid cells are in thermal interaction with the PCM cells via the wall cells. This structure resembles the tank's internal scheme from Figure 3.

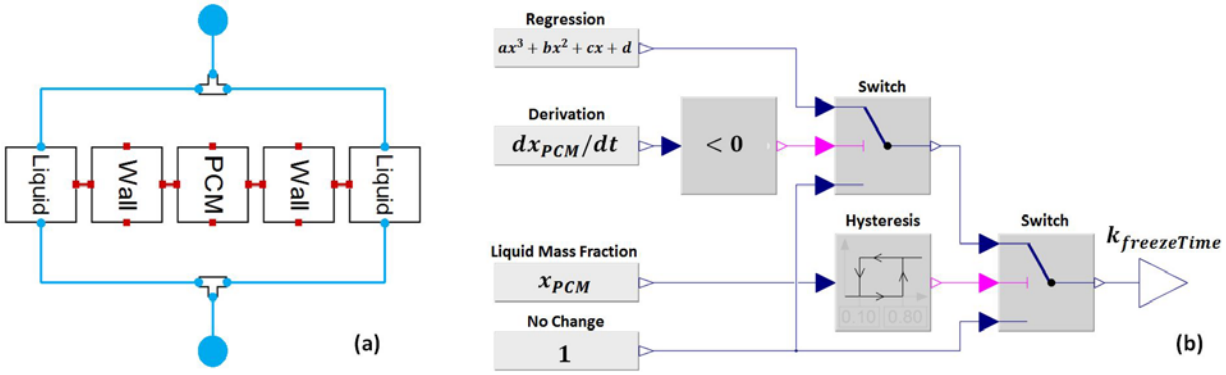

Figure 4 – (a) Internal interface of the PCM heat exchanger model. The blue dots denote the input and output source of water, while red dots denote heat ports. (b) Model to calculate the freezing time factor.

3.2.1 Liquid cell: The energy balance equation for the liquid cell is given as

$$m_{water} \cdot c_p \cdot \frac{dT_{water}}{dt} = \dot{m}_{in} \cdot h_{in} + \dot{m}_{out} \cdot h_{out} + \dot{Q}_{water} \quad (1)$$

The heat transfer rate $\dot{Q}$ in each cell is dependent on the type of heat transfer. For the present case, three different types of heat transfer are possible: conduction, natural convection or forced convection. Whether the dominating type of heat transfer is conduction or convection, can be deduced from the Rayleigh number (Ra), a dimensionless number in fluid mechanics. Computing Ra for several possible boundary conditions for the present case lead always to Ra > 1700, which indicates that forced convection is the dominant heat transfer type for the liquid cell. The heat transfer rate for forced convection is

$$\dot{Q}_{water} = \alpha_{water} \cdot A \cdot (T_{port} - T_{water}) \cdot \left(\frac{Pr}{Pr_{atWall}}\right)^{0.25} \quad (2)$$

The last factor in Eq. (2) is a function of the Prandtl number Pr and considers the change of thermophysical properties of water as a result of a changing temperature between the water directly at the wall and in the middle of the flow channel (VDI 2013). Finally, the heat transfer coefficient α_{water} was estimated for the PCM heat exchanger. The best correspondence with experimental data was obtained assuming the case "flow over a horizontal plane", in which case the heat transfer coefficient is calculated as (VDI 2013)

$$\alpha_{water} = k_{freeze\ time} \frac{\lambda \cdot Nu}{l_{flow\ channel}} \quad (3)$$

The freezing time factor $k_{freeze\ time}$ is considering the effect, that the time for freezing the PCM is greater than the time for melting the PCM. This factor is discussed in more detail in section 3.2.3.

3.2.2 Wall cell: The energy balance equation for the wall cell is:

http://dx.doi.org/10.18462/iir.nh3-co2.2017.0039

$$m_{wall} * c_p * \frac{dT_{wall}}{dt} = \dot{Q}_{wall,portN} + \dot{Q}_{wall,portS} + \dot{Q}_{wall,portW} + \dot{Q}_{wall,portE} \quad (4)$$

While the liquid cell is in thermal interaction only with the adjacent wall cell, the wall cell possesses four such interaction points, known as heat ports (red dots in Figure 4(a)). Two of them are connected to the liquid cell (port "S") and the PCM cell ("N"). The remaining two side-ports are connected to the previous ("W") and next wall cell ("E"), if the discretization $n_{cells,flow\ channel} > 1$.

For the wall cell, the heat transfer type is clearly only heat conduction. The respective heat transfer rates are calculated for each heat port separately:

$$\dot{Q}_{wall,portX} = \frac{T_{portX} - T_{wall}}{R_X} \quad (5)$$

Where R_X is the thermal resistance in $K \cdot m/W$. The subscripts refer to the direction, i.e. the particular cross-section areas for calculating the thermal resistance: in the direction of the length (west-east, *WE*) and in the direction of the width (north-south, *NS*) of the tank. Thus, R_{NS} is the thermal resistance for the heat transfer between water and PCM, and R_{WE} for the heat transfer between successive wall cells:

$$R_{NS} = \frac{d_{wall}/2}{\lambda_{HDPE} * A_{NS}} \quad (6)$$

$$R_{WE} = \frac{l_{WE}/2}{\lambda_{HDPE} * A_{WE}} \quad (7)$$

3.2.3 PCM Cell: The energy balance equation for the PCM cell is:

$$m_{PCM} * \frac{dh_{PCM}}{dt} = \dot{Q}_{PCM,portN} + \dot{Q}_{PCM,portS} + \dot{Q}_{PCM,portW} + \dot{Q}_{PCM,portE} \quad (8)$$

The main difference to the balance equations of the liquid and wall cells is the use of time dependence (derivation) of enthalpy instead of temperature. This was done because calculation of thermal capacity c_p in the area of phase change is nontrivial.

Furthermore, determining the type of heat transfer within the PCM cell is not straightforward. In the case of a completely frozen PCM, the heat transfer will be conduction only. However, as soon as some of the PCM has melted, the liquid PCM will start to move within the container due to temperature differences within the cell, creating natural convection. At the same time, the thermal conductivity, λ, will alter with the changing phase and liquid mass fraction, x. In the case of an entirely molten PCM container, the temperature of the liquid at the wall will increase, changing its thermophysical properties and affecting the heat transfer. Finally, the most challenging case is the beginning of freezing. The emerging and increasing layer of frozen PCM directly at the wall acts as an insulator for the remaining liquid. As a result, the freezing time of a PCM container is higher than the melting time.

For simplification, for the model utilized in this study, it was assumed that the heat transfer type is merely heat conduction. Thus, the applied equations for the PCM cell are analogous to the equations applied to the wall cell (Eqs. (5) – (7)). To take into account the difference between melting and freezing time, a freezing time factor, $k_{freeze\ time}$, was introduced in the heat transfer coefficient for the liquid cell (Eq. (3)). The factor was implemented into the liquid cell instead of the PCM cell, because it was easier to affect the model's performance by changing the heat transfer coefficient of the liquid than by changing the thermal resistance of the PCM. With this approach, the progressing freezing of the PCM cell affects directly the heat transfer coefficient of water.

The factor $k_{freeze\ time}$ is a function of the liquid mass fraction of the PCM, *x*. To compute $k_{freeze\ time}$, a polynomial regression function is used:

$$k_{freeze\ time} = f(x_{PCM}) = ax_{PCM}^3 + bx_{PCM}^2 + cx_{PCM} + d \quad (9)$$

The parameters for the regression function were adjusted such that the heat transfer coefficient becomes smaller when the molten PCM starts to freeze. Figure 4 (b) shows how $k_{freeze\ time}$ is calculated in the model. Most of the time, $k_{freeze\ time}$ equals one. It will decrease to a lower value (< 1) and thus start to slow down the heat transfer rate as soon as $\frac{dx}{dt}$ becomes negative, which implies the start of freezing. As discussed before, the

http://dx.doi.org/10.18462/iir.nh3-co2.2017.0039

freezing process of the PCM leads to an increasing layer of frozen PCM at the container wall, hindering the heat transfer. However, to keep $k_{freeze\ time}$ from delaying the process every single time a partial or only transient freezing occurs, hysteresis was included in the model to ensure the factor $k_{freeze\ time}$ is effective only when it is actually required.

4. VALIDATION OF THE MODEL

In this section, the simulation results are compared with measurement data to assess the accuracy of the PCM storage model, as well as to adjust the freezing time factor. First, melting and freezing profiles provided by the PCM manufacturer are compared with simulated profiles, at a constant mass flow and inlet temperature. In a subsequent validation step, measurement data from the PCM storage at the Bergen University College is utilized in order to evaluate the dynamic response of the model under varying mass flow rate and inlet temperature.

4.1 Freezing and melting profiles

Freezing and melting profiles describe the general performance of a PCM during the phase change processes, and are unique to each PCM and PCM container shape. Figure 5 compares the measured and simulated freezing and melting profiles as a function of the temperature difference of the supplied water and the PCM. From Figure 5 it can be seen that the freezing and melting time decreases with increasing temperature difference.

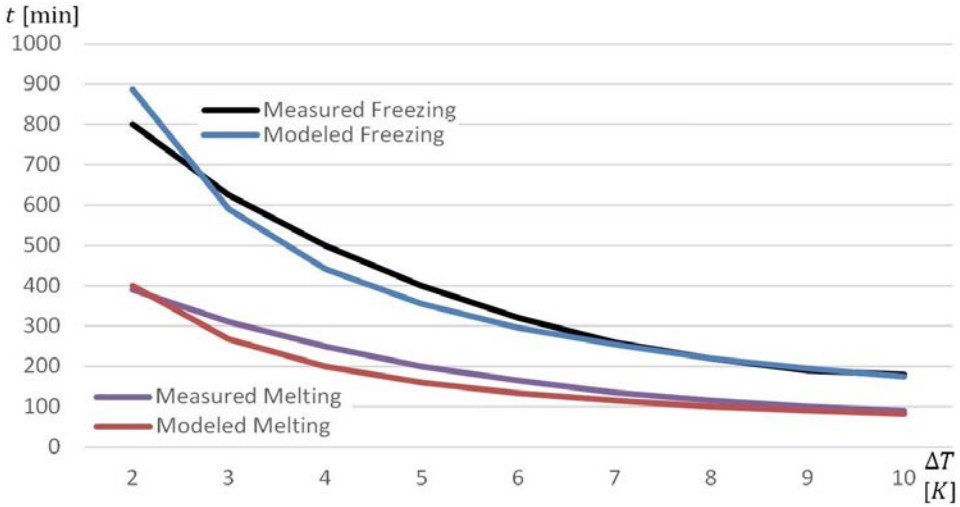

Figure 5 – Measured (PCM Products Ltd. 2011) and simulated freezing and melting times as a function of temperature difference between the supplied water and the PCM

Based on Figure 5, the model is capable of estimating the correct profiles for the freezing and melting times. Unfortunately, no information was available about the mass flow that was applied when the measured profiles were recorded. However, as shown in section 3, the heat transfer coefficient is a function of the Reynolds number and thus the mass flow rate. The mass flow rate for the model was set to 10 m^3/h, a value taken from the data sets recorded at Bergen University College. The freezing and melting profiles could hence be utilized only for a preliminary validation; to check that the model was able to reproduce the trajectories for freezing and melting. Furthermore, the freezing and melting profiles were applied to adjust the parameters of the regression function for calculating the freezing factor, $k_{freeze\ time}$ (Eq. (9)). Without the freezing factor the profiles for freezing and melting time would be almost equal.

4.2 Measurement data from Bergen University College

Measurement data for the mass flow rate and inlet temperature, as well as measured and modelled results for the outlet temperature and heat flow rate from the PCM-TES at the Bergen University College during 30.05. - 01.06.2016 are shown in Figure 6. In order to fully melt the PCM tank, and hence to be able to properly study the freezing and melting characteristics, only one tank was employed in the measurements.

http://dx.doi.org/10.18462/iir.nh3-co2.2017.0039

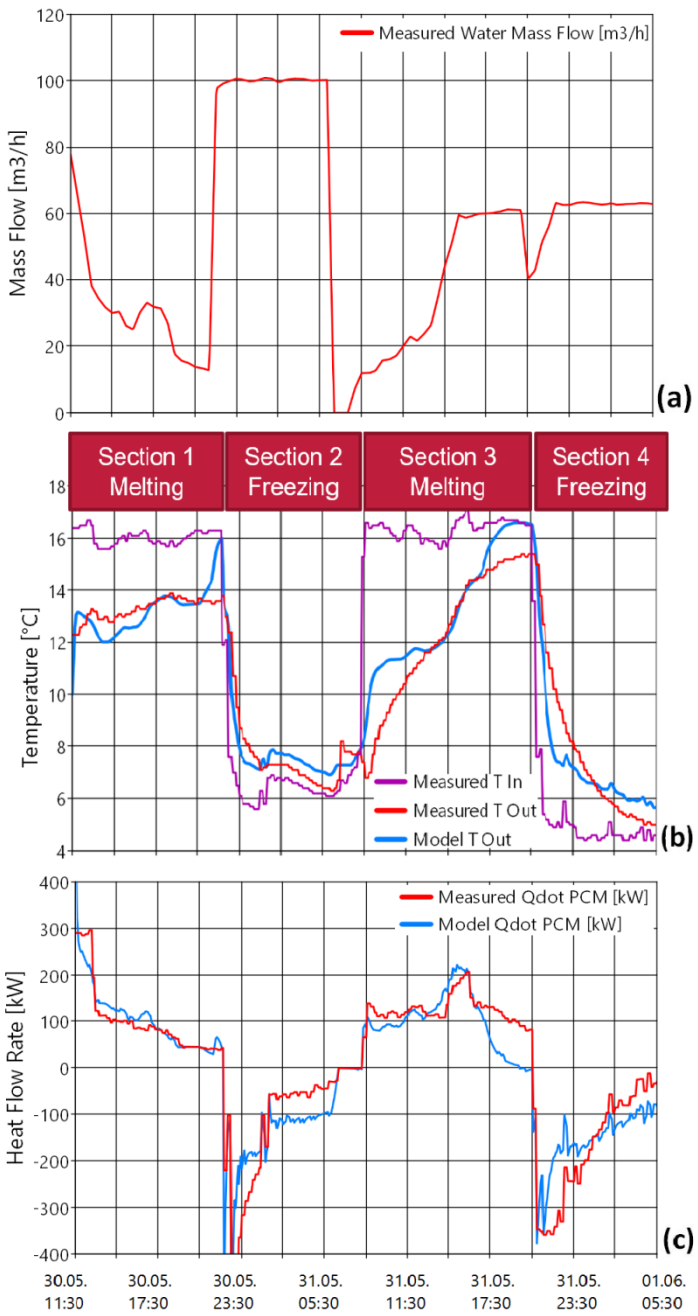

Figure 6 – (a) Measured mass flow rate through the PCM tank; (b) measured inlet and outlet temperature together with the simulated outlet temperature; and (c) measured and simulated heat transfer rate for the period 30.05.-01.06.2016.

Apart from a very short period in the middle of the measurement period, the mass flow was constantly higher than zero (Figure 6 (a)). The inlet water temperature was varying between 16 °C for the melting sections and 5-6 °C for the freezing sections (Figure 6 (b)). The model is capable of reproducing the overall profile of the measured outlet temperature.

The largest deviations between the measured and calculated outlet temperature and heat transfer rate occur during melting (sections 1 and 3 in Figure 6 (b)). The simulated outlet temperature deviates from the measured values particularly at the beginning and at the end of these sections. A reason might be that the freezing factor $k_{freeze\ time}$ introduced in section 3 only considers the effect of the freezing process on the heat transfer coefficient. Based on Figures 6 (b) and (c), it seems that the heat transfer coefficient is influenced by the melting process as well, but in a different way than by the freezing process. Thus, a factor describing the melting behaviour should be included in the model in the future.

During freezing (sections 2 and 4 in Figure 6 (b)), the model is able to reproduce the measured profiles fairly well. Despite the small deviations between the measured and calculated profiles for the outlet temperature and heat transfer rate in these sections, the accumulated values for heat transfer are very similar: 1113 kWh/1235 kWh for measured/calculated total heat transfer in section 2 and 1618 kWh/1621 kWh in section 4. For melting, the deviation is slightly bigger; the accumulated values for the measured/simulated heat transfer are 1103 kWh/1164 kWh for section 1 and 1536 kWh/1269 kWh for section 3.

5. CONCLUSIONS

A model for simulating the performance of a PCM-TES has been derived in the dynamic simulation program Dymola. The model was validated using measurement data from an existing PCM cold storage system at the Bergen University College. The aim with the model was to gain understanding of the charging and discharging dynamics of the PCM storage, and to enable better dimensioning of similar storage systems and design of the operation modes in the future.

http://dx.doi.org/10.18462/iir.nh3-co2.2017.0039

The model was capable of predicting the measured values correctly at an adequate accuracy. In particular, the accumulated values for the amount of heat absorbed or released by the PCM storage were very similar as given by measurements and the model. However, further model refinement is required to be able to properly reproduce the profiles for the outlet temperature and heat transfer rate.

The deviations in the simulation results with respect to the measurement data can be assigned to the assumptions that were made while deriving the present model with regards to the influence of the phase change on the heat transfer processes. The change in the heat transfer coefficient with progressing melting or freezing within the PCM containers needs to be modelled in a more accurate way by implementing proper equations and correlations.

ACKNOWLEDGEMENTS

The authors would like to acknowledge the support from The Research Council of Norway, grant no 228656/E20 INTERACT, and the industrial partner SWECO for providing the measurement data from Bergen University College.

NOMENCLATURE

TES	Thermal Energy Storage	PCM	Phase Change Material
α	Heat Transfer Coefficient [$Wm^{-2}K^{-1}$]	λ	Therm. Cond. [$Wm^{-1}K^{-1}$]
A	Cross-Sectional Area [m^2]	d	Container Wall Thickness [m]
l	Flow Channel Length [m]	Nu	Nusselt-Number [-]
Pr	Prandtl-Number [-]	$\dot{Q}$	Heat Flow Rate [W]
R	Thermal Resistance [mKW^{-1}]	x	Liquid Mass Fraction [-]
Subscripts			
in	At Inlet	out	At Outlet
NS	In the Direction of the Heat Flow	WE	Direction Perpendicular to the Heat Flow

REFERENCES

1. Dar, U. 2014, Høgskolen i Bergen Energisentral, SWECO.
2. Hed, G. and R. Bellander, 2006, Mathematical modelling of PCM air heat exchanger, *Energy and Buildings* **38**(2): 82-89.
3. Liu, L., D. Su, Y. Tang and G. Fang, 2016, Thermal conductivity enhancement of phase change materials for thermal energy storage: A review, *Renewable and Sustainable Energy Reviews* **62**: 305-317.
4. PCM Products Ltd. 2011, PlusICE Phase Change Materials, Retrieved 11.12.2014, from http://www.pcmproducts.net/files/thermal_storage_catalogue.pdf.
5. Pérez-Lombard, L., J. Ortiz and C. Pout, 2008, A review on buildings energy consumption information, *Energy and buildings* **40**(3): 394-398.
6. Regin, A. F., S. Solanki and J. Saini, 2008, Heat transfer characteristics of thermal energy storage system using PCM capsules: a review, *Renewable and Sustainable Energy Reviews* **12**(9): 2438-2458.
7. TLK-Thermo GmbH. 2016, TLK-Thermo – Engineering Services and Software for Thermal Systems, from https://www.tlk-thermo.com/index.php/en/.
8. VDI, 2013, VDI Heat Atlas, Verein Deutscher Ingenieure (VDI), VDI-Gesellschaft (GVC).